Seven Years of Structure Functions

Keith Griffioen
College of William & Mary

Highlights of the First Seven Years
Jefferson Lab Users Meeting
12 June 2003

- Introduction
- Unpolarized structure functions
- Tagged structure functions
- g_1, asymmetries, and g_2
- Moments
- Conclusions

Kinematics

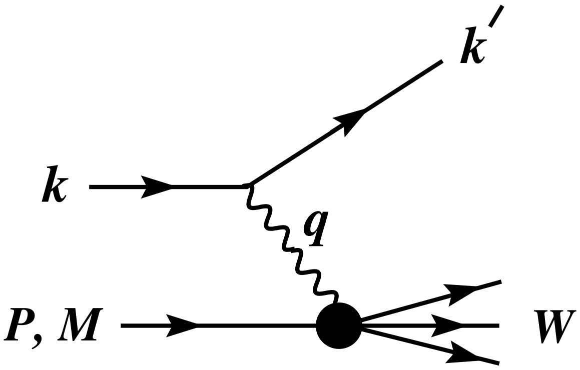

Lepton scattering is described by two variables θ and E', or Lorentz invariant combinations.
k and k' are incident and final lepton 4-momenta.
p is the initial nucleon 4-momentum.
q is the 4-momentum of the transferred virtual photon.
s_N and s_ℓ are nucleon and lepton spin 4-vectors.
M is the nucleon mass

$$\frac{d^2\sigma}{dE'd\Omega} = \frac{e^4}{16\pi^2 Q^4}\left(\frac{E'}{E}\right) L^{\mu\nu}W_{\mu\nu}$$

$$L^{\mu\nu} = 2\left[k'^{\mu}k^{\nu} + k'^{\nu}k^{\mu} - k\cdot k' g^{\mu\nu} - i\epsilon^{\mu\nu\rho\sigma}q_\rho s_{\ell\sigma}\right]$$

$$q^\mu W^{\mu\nu} = q^\nu W_{\mu\nu} = q_\mu L^{\mu\nu} = q_\nu L^{\mu\nu} = 0$$

$$W_{\mu\nu} = -F_1 g_{\mu\nu} + \frac{F_2}{p\cdot q}p_\mu p_\nu + \frac{ig_1}{p\cdot q}\epsilon_{\mu\nu\rho\sigma}q^\rho s_{N\sigma} + \frac{ig_2}{(p\cdot q)^2}\epsilon_{\mu\nu\rho\sigma}q^\rho(p\cdot q s_{N\sigma} - s_N\cdot q p^\sigma)$$

Kinematics

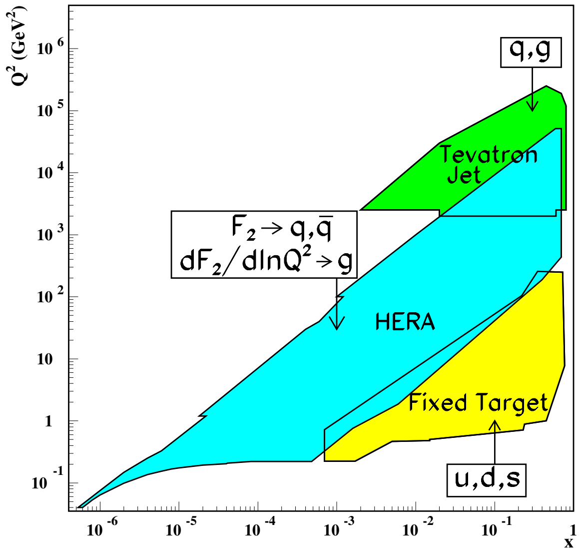

Lorentz invariants:

$\nu = p \cdot q/M = (E - E')_{\mathrm{lab}}$

$Q^2 = -q \cdot q = (4EE' \sin^2 \frac{\theta}{2})_{\mathrm{lab}}$

$x = -q \cdot q/2p \cdot q = (Q^2/2M\nu)_{\mathrm{lab}}$

$y = p \cdot q/p \cdot k = (\nu/E)_{\mathrm{lab}}$

$W^2 = (p+q)^2 = (M^2 + 2M\nu - Q^2)_{\mathrm{lab}}$

$s = (k+p)^2 = (2EM + M^2)_{\mathrm{lab}}$

$$\frac{d^2\sigma}{dx dQ^2} = \frac{\pi\nu}{xE'E}\frac{d^2\sigma}{dE'd\Omega}$$

Variables of choice are (x, Q^2) for DIS and (W, Q^2) for resonance region.

Structure Functions

Unpolarized Cross Section:

$$\frac{d^2\sigma}{dxdQ^2} = \frac{8\pi\alpha^2 y}{Q^4}\left[\frac{y}{2}F_1 + \frac{\xi}{2xy}F_2\right]$$

Polarized Cross Section:

$$\begin{aligned}\frac{d^2\Delta\sigma}{dxdQ^2} \;=\; & \frac{8\pi\alpha^2 y}{Q^4}[\cos\alpha\{(\xi+\frac{y}{2})g_1 - \frac{\gamma y}{2}g_2\} - \\ & \sin\alpha\cos\phi\{\frac{y}{2}g_1 + g_2\}]\end{aligned}$$

α = polar angle of target spin wrt the beam axis
ϕ = azimuthal spin angle wrt the scattering plane
$\alpha = 0°$ (longitudinal); $\alpha = 90°, \phi = 0°$ (transverse).
$\gamma^2 = 4M^2x^2/Q^2 = Q^2/\nu^2$
$\xi = 1 - y - \gamma y^2/4$

Parton Model:
$F_1(x,Q^2) = \frac{1}{2}\Sigma_i e_i^2(q^\uparrow(x) + q^\downarrow(x) + \bar{q}^\uparrow(x) + \bar{q}^\downarrow(x))$
$F_2(x,Q^2) = 2xF_1(x,Q^2)$
$g_1(x,Q^2) = \frac{1}{2}\Sigma_i e_i^2(q^\uparrow(x) - q^\downarrow(x) + \bar{q}^\uparrow(x) - \bar{q}^\downarrow(x))$
$g_2(x,Q^2) = 0$

World Data on F_2

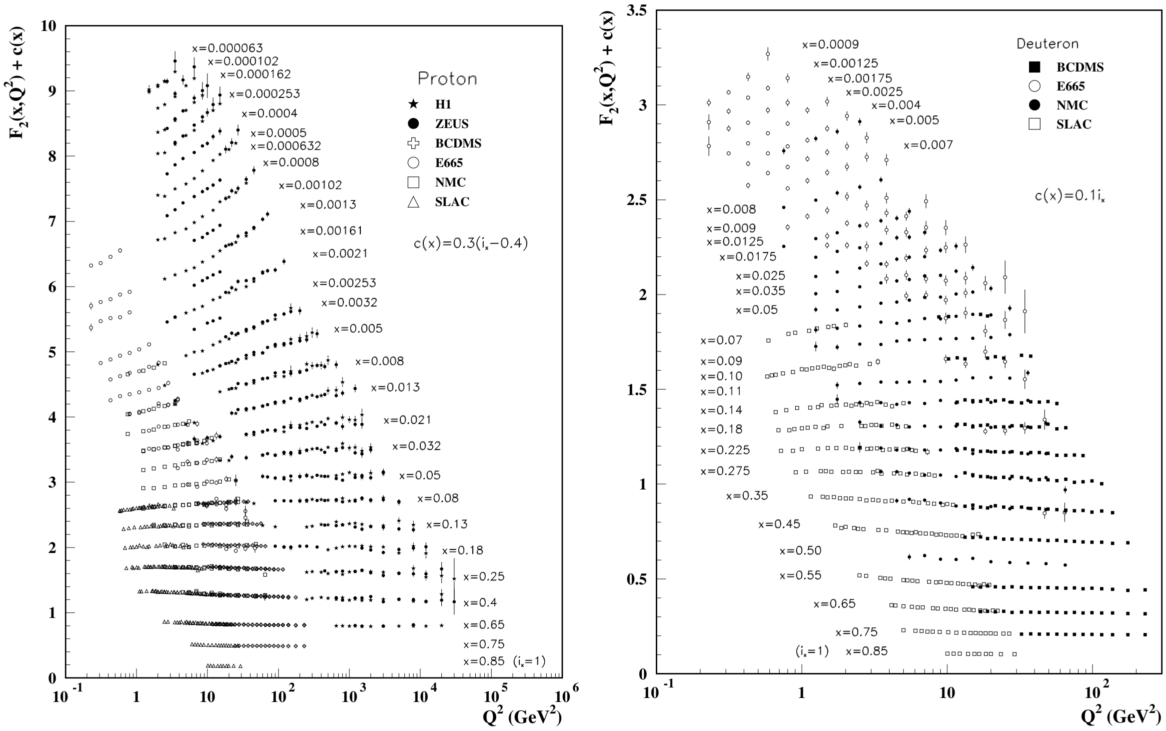

- $F_2(x)$ is not constant with Q^2, but exhibits scaling violations.

- Our microscope has resolution $1/Q$, and sees the corresponding QCD fur of quarks and gluons surrounding the bare quark.

- DGLAP equations describe QCD evolution of parton distributions: $\partial q_i(x, Q^2)/\partial \ln Q^2 \sim \frac{\alpha_s(Q^2)}{2\pi} \int_x^1 \frac{dy}{y} P(y) \times q_i(\frac{x}{y}, Q^2)$ in which $P(y)$ is the probability of a given parton splitting into two others.

PDF

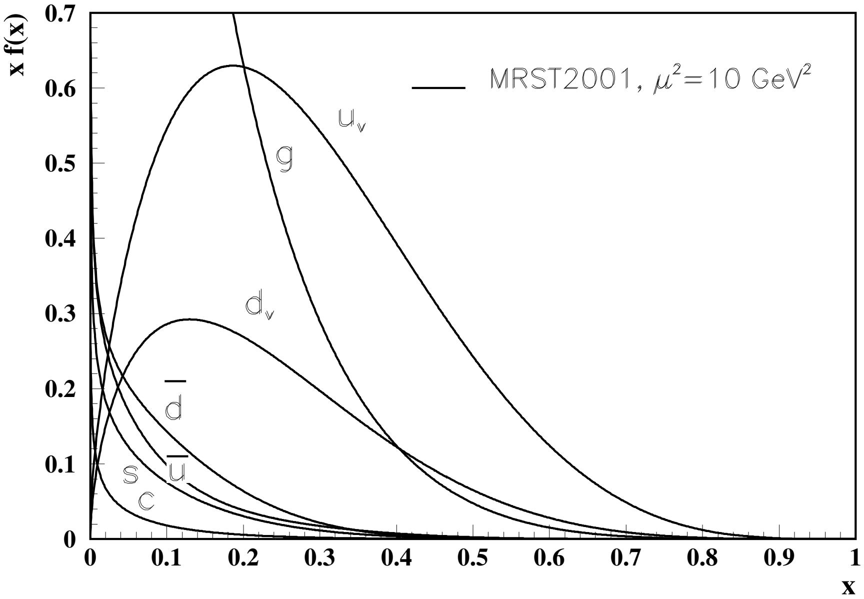
x f(x)
0.7
0.6
0.5
0.4
0.3
0.2
0.1
0
0
0.1
0.2
0.3
0.4
0.5
0.6
0.7
0.8
0.9
1
x
MRST2001, μ^2=10 GeV^2
u_v
g
d_v
$\bar{d}$
$\bar{u}$
s
c

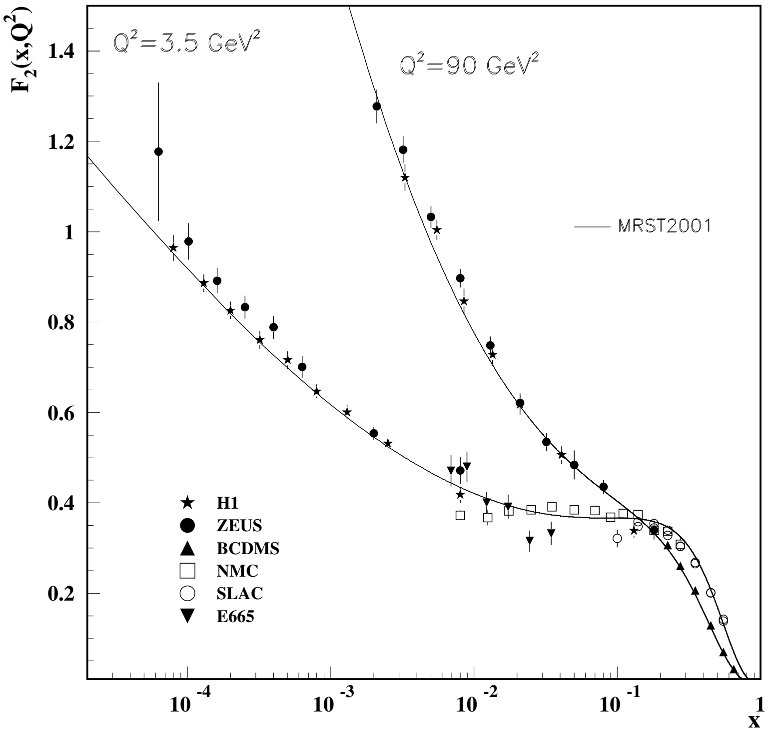
$F_2(x,Q^2)$
1.4
1.2
1
0.8
0.6
0.4
0.2
10^{-4}
10^{-3}
10^{-2}
10^{-1}
1
x
Q^2=3.5 GeV^2
Q^2=90 GeV^2
MRST2001
H1
ZEUS
BCDMS
NMC
SLAC
E665

R and FL

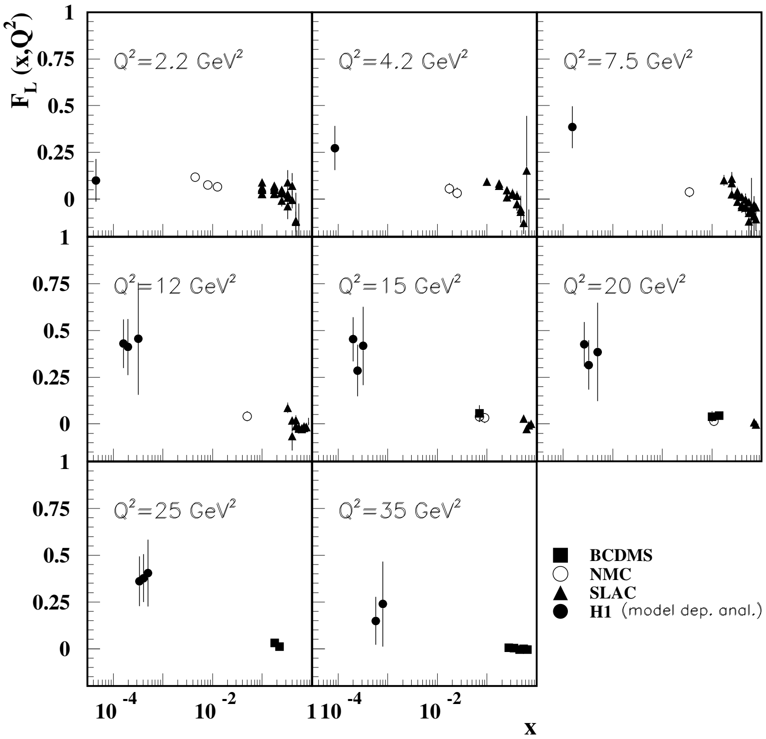

- $R(x, Q^2) = \sigma_L/\sigma_T = (1 + \gamma^2)F_2/2xF_1 - 1$
- $F_L(x, Q^2) = (1 + \gamma^2)F_2 - 2xF_1$
- Virtual photon polarization vectors for $q_\mu = (q_0, 0, 0, q_3)$ are $\epsilon^\mu_\pm = \frac{1}{\sqrt{2}}(0, \mp 1, -i, 0)$ for $\pm$ helicity (transverse), and $\epsilon^\mu_0 = \frac{1}{Q}(q^3, 0, 0, q^0)$ (longitudinal).
- Both F_L and R vanish in the parton model.

Hall C: E94-110

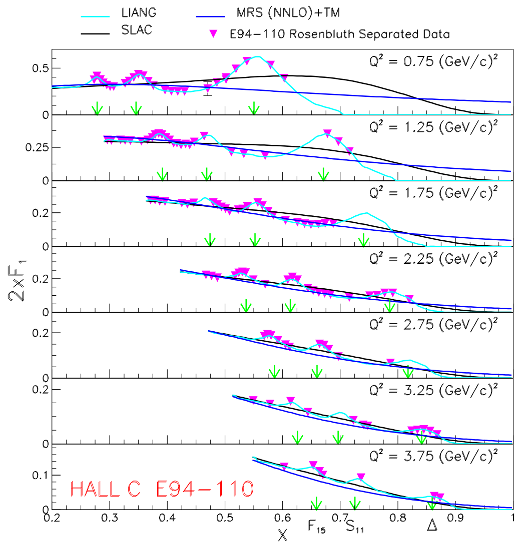

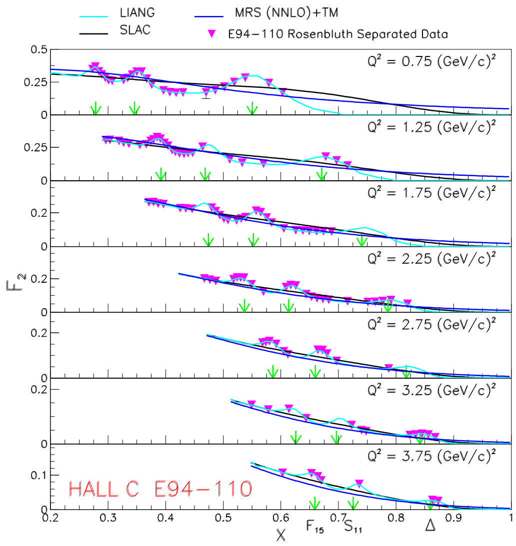

$$\frac{d^2\sigma}{dE'd\Omega} = \Gamma_V(\sigma_T + \epsilon\sigma_L)$$

$1/\epsilon = 1 + 2(1 + 1/\gamma^2)\tan^2\frac{\theta}{2}$
$\sigma_T = (\sigma^T_{1/2} + \sigma^T_{3/2})/2 = NF_1$
$\sigma^T_{1/2} = N(F_1 + g_1 - \gamma^2 g_2) \propto |A_{1/2}|^2$
$\sigma^T_{3/2} = N(F_1 - g_1 + \gamma^2 g_2) \propto |A_{3/2}|^2$
$\sigma^L_{1/2} = \sigma_L = NF_L/2x \propto |S_{1/2}|^2$
$\sigma^{LT}_{1/2} = \sigma_{LT} = N\frac{Q}{M\nu}(g_1 + g_2) \propto S^*_{1/2}A_{1/2}$
$N = \frac{4\pi^2\alpha}{KM}$
$\Gamma_V = \frac{\alpha K E'}{2\pi^2 Q^2 E(1-\epsilon)}$

Rosenbluth separation gives σ_T and σ_L separately.

Hall C: E94-110

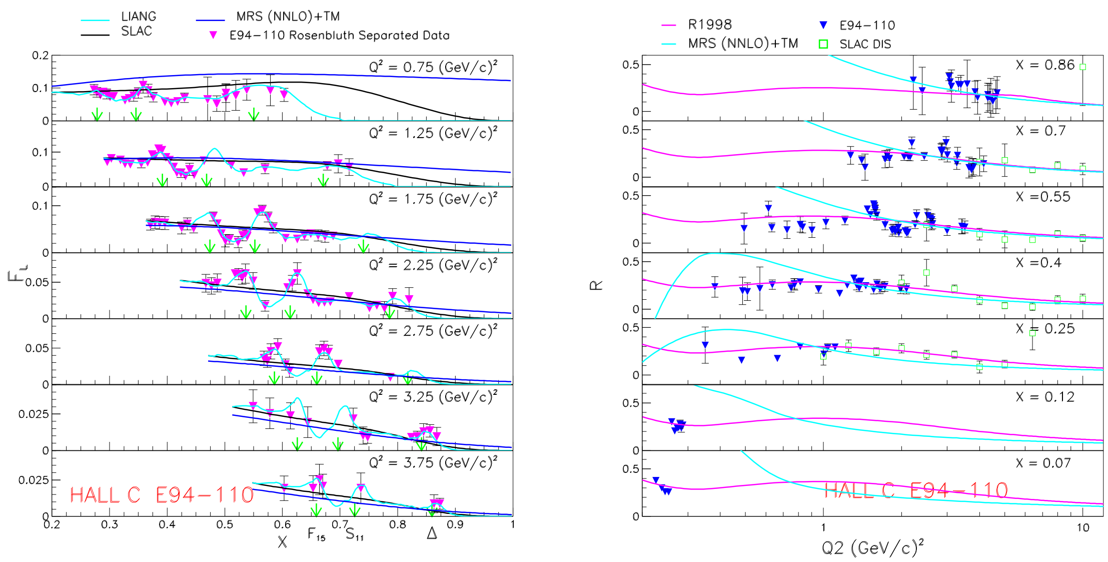

- Both F_L and R are positive and get smaller slowly with Q^2.
- Resonances show up as bumps that move with x as Q^2 increases.
- New global parametrization fits the Q^2 dependence for each bin in W.
- DIS extrapolations do well on average in the resonance region (duality).
- The DIS R1998 fit to R does extremely well with the new data, whereas NNLO extrapolations fail.

Hall C: E94-110

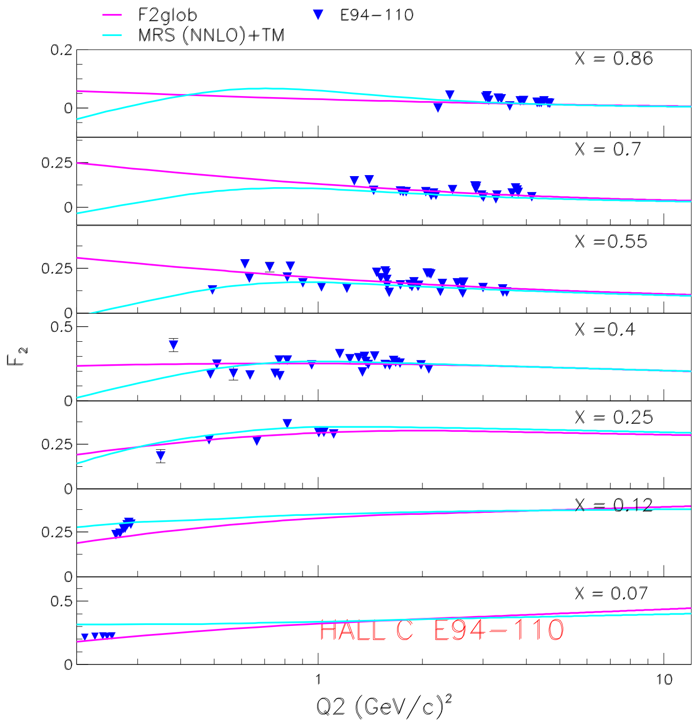

- Old SLAC parametrization does well.
- NNLO QCD fit also generally agrees with the Q^2 dependence when corrected for target-mass effects.
- Data at low Q^2 are often plotted versus Nachtmann $\xi = 2x/(1+\sqrt{1+4M^2x^2/Q^2})$ to correct for target-mass. Because there are scaling violations at all Q^2, one might prefer to use (x, Q^2) consistently.

DIS Hadron Tagging

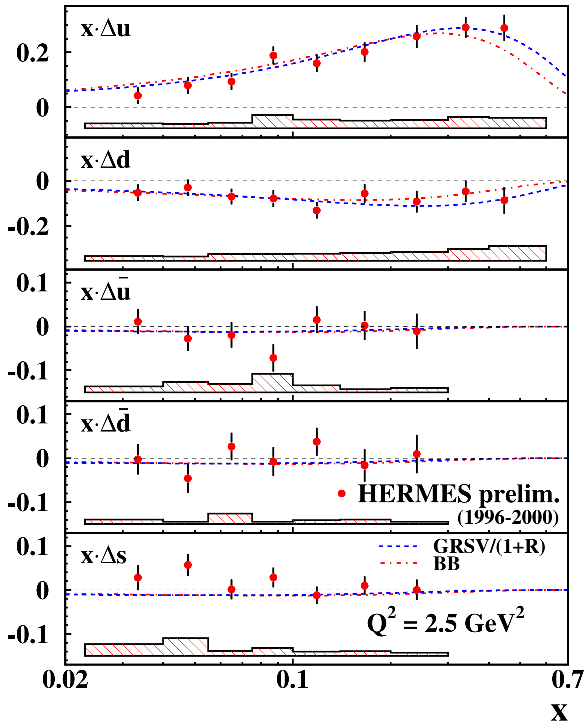

$$\sigma^h(x, Q^2, z) \propto \Sigma_i\, e_i^2 q_i(x, Q^2) D_i^h(z, Q^2);\, z = E_h/\nu$$

$$g_1/F_1 = \frac{\Sigma_i\, \Delta q_i(x, Q^2) \int_{z_{\rm min}}^{z_{\rm max}} dz D_i^h(z, Q^2)}{\Sigma_i\, q_i(x, Q^2) \int_{z_{\rm min}}^{z_{\rm max}} dz D_i^h(z, Q^2)}$$

$\Delta q/q$ extracted from semi-inclusive data, given knowledge of the fragmentation functions D_i^h.

- Data from HERMES
- CLAS eg1 will also be able to do this analysis.

Tagging with a π: Isospin Differences

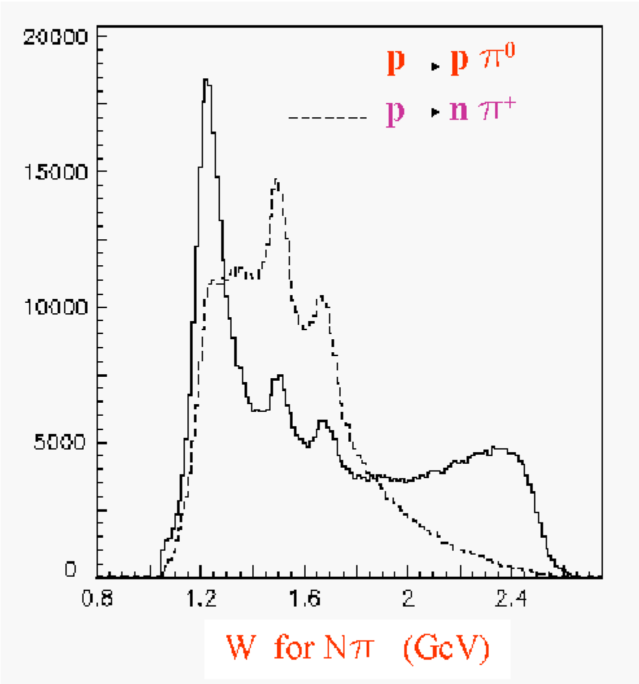

- Raw counts for $ep \to ep\pi^0$ and $ep \to en\pi^+$
- $$|\frac{3}{2}\frac{1}{2}\rangle = \sqrt{\frac{1}{3}}|n\pi^+\rangle + \sqrt{\frac{2}{3}}|p\pi^0\rangle$$
  $$|\frac{1}{2}\frac{1}{2}\rangle = \sqrt{\frac{2}{3}}|n\pi^+\rangle - \sqrt{\frac{1}{3}}|p\pi^0\rangle$$
- $p\pi^0$ emphasizes isopin $T = \frac{3}{2}$ states
- $n\pi^+$ emphasizes isopin $T = \frac{1}{2}$ states

$A_1 + \eta A_2$ **versus** Q^2 **from** $\pi^+ n$

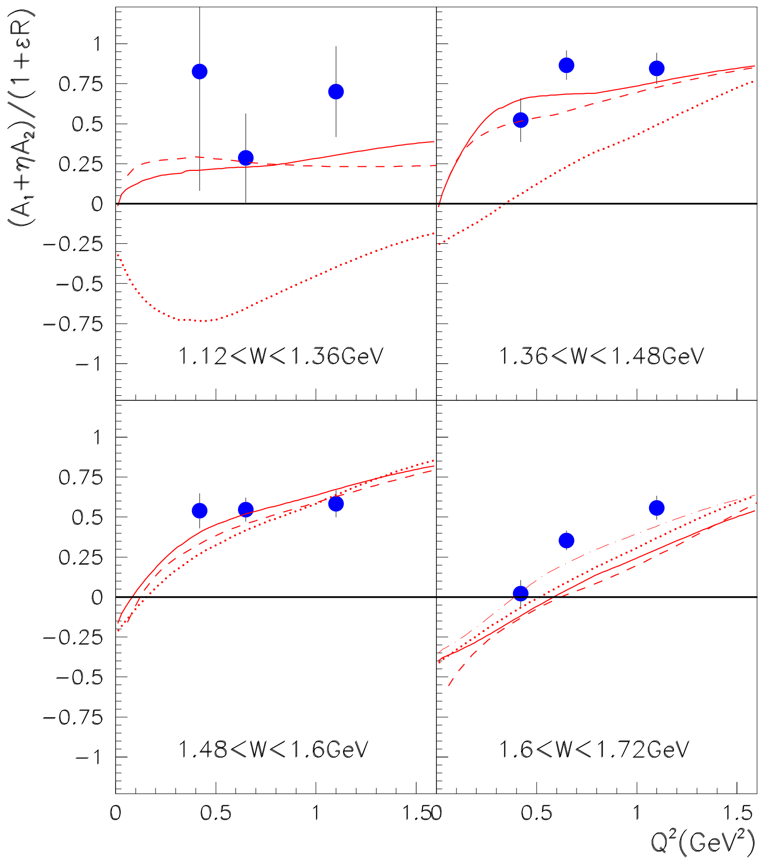

- Integrated over $\cos\theta^*$
- AO resonance (dotted) [PRD47(93)46]
- AO full (solid)
- AO with A_1^{F15} increased by 0.4 (dot-dashed)
- MAID2000 [NPA645(99)145]

CLAS E94-102: $d(e, e'p_s)$

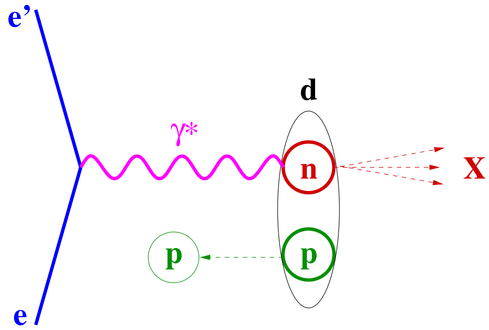

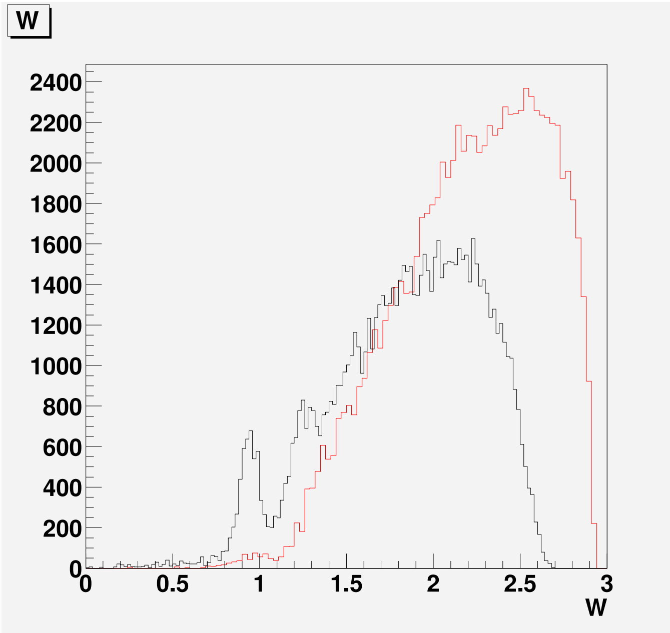

- At 6 GeV, CLAS can measure into the deep-inelastic region.
- Measures the neutron structure function for high ($>$ 250 MeV/c) momentum spectators; study off-shell effects and modifications to the structure functions when two nucleons are close
- Red curve: inclusive data from the deuteron target with elastic and resonances smeared out.
- Black curve: $(e, e'p_s)$ data corrected for the neutron momentum before scattering. Peaks appear!

CLAS E03-012: BONUS

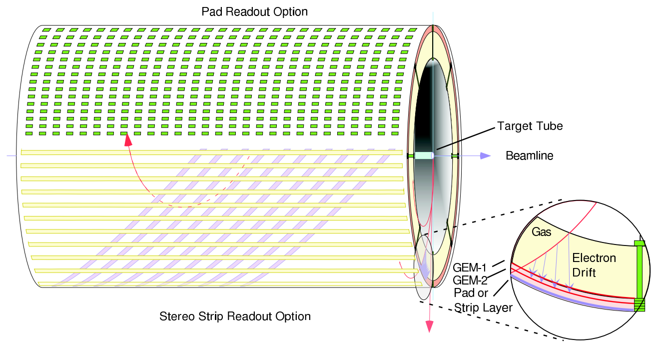

- Low-energy proton spectators from deuterium are hard to detect because of energy loss in the target.
- Slow spectators imply the neutron and proton are on average far apart (barely bound).
- Tagging slow protons from deuterium allows one to create a nearly free neutron target.
- Gaseous deuterium target; radial time projection chamber; gas electron multiplier (GEM) readout.

CLAS BONUS

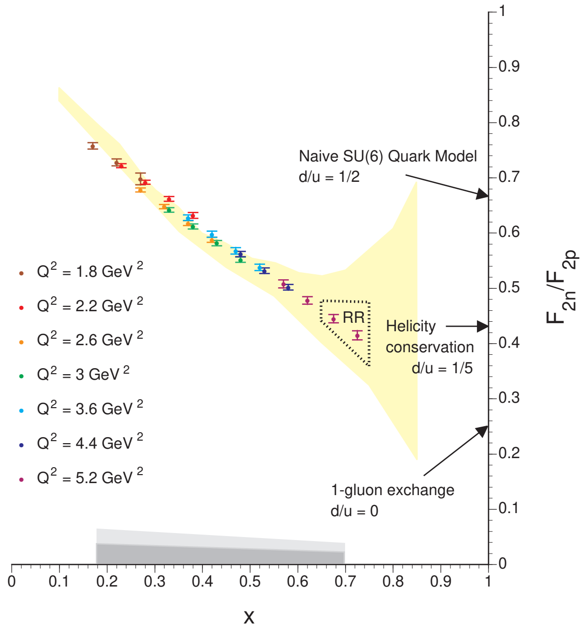

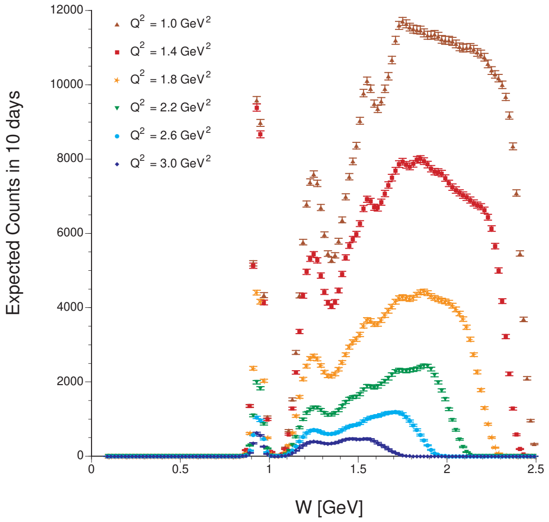

- Tagged structure functions corrected for nucleon motion show sharp peaks for elastic and resonances (right curve, expected results).
- Barely Offshell NUcleon Structure (BONUS) experiment will measure neutron structure functions without the usual proton contamination and smearing from deuterium.
- This method is especially useful at high x where model uncertainties dominate the extraction of F_2^n.
- This technique is easily extended to 12 GeV beams.

$g_1(x, Q^2)$

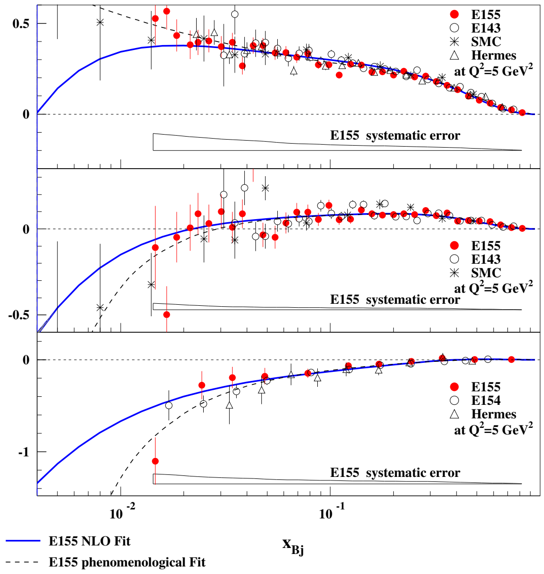

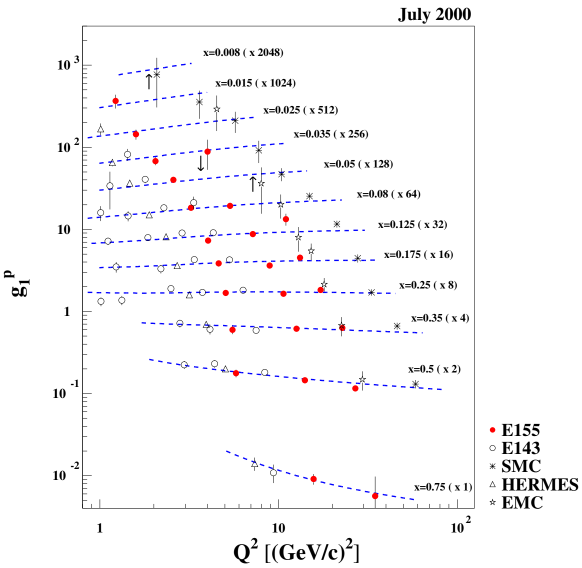

$$\left(\frac{d^2\Delta\sigma}{dE'd\Omega}\right)_{\parallel} = 2\Gamma_V D(1+\epsilon R)[\sigma_{TT} + \eta\sigma_{LT}]$$

$$\left(\frac{d^2\Delta\sigma}{dE'd\Omega}\right)_{\perp} = 2\Gamma_V d(1+\epsilon R)[\sigma_{LT} - \zeta\sigma_{TT}]$$

D and d are depolarization factors.
η and ζ are kinematic factors (small).
$\sigma_{TT} = (\sigma^T_{1/2} - \sigma^T_{3/2})/2 = N(g_1 - \gamma^2 g_2)$.

- Both $\parallel$ and $\perp$ data are necessary to extract g_1
- Q^2 evolution similar to the unpolarized case.
- Consistent NLO analysis of world's data: $\Delta\Sigma = 0.23 \pm 0.07$ and $\Delta G = 1.6 \pm 0.8 \pm 1.1$

CLAS (eg1a) g_1^p vs. x

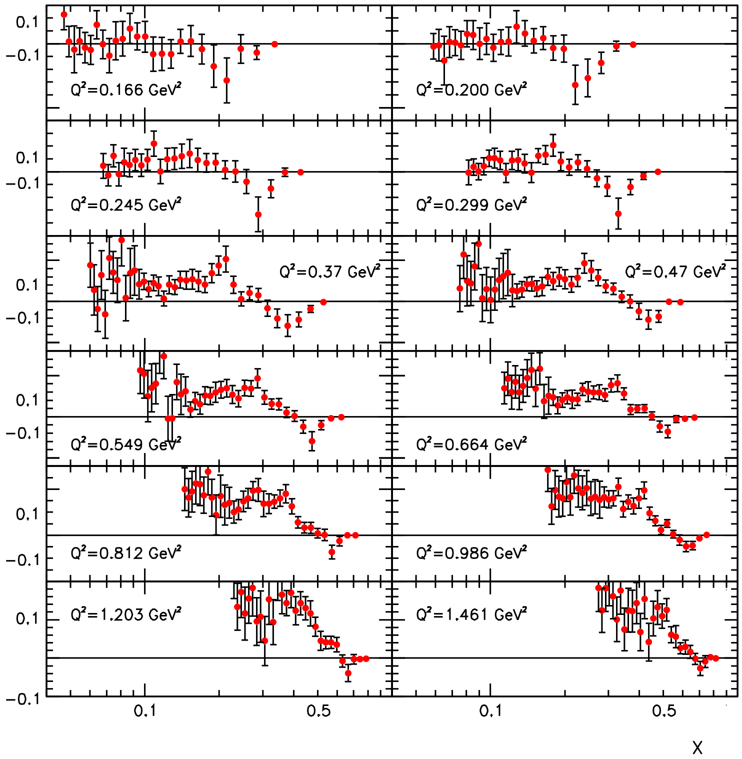

- CLAS has extended the measurements of g_1 into the resonance region.
- The Δ resonance, which moves upward in x with increasing Q^2, drives g_1 negative.
- By comparison, g_1 is always positive for DIS.

CLAS (eg1b) g_1^p vs. x

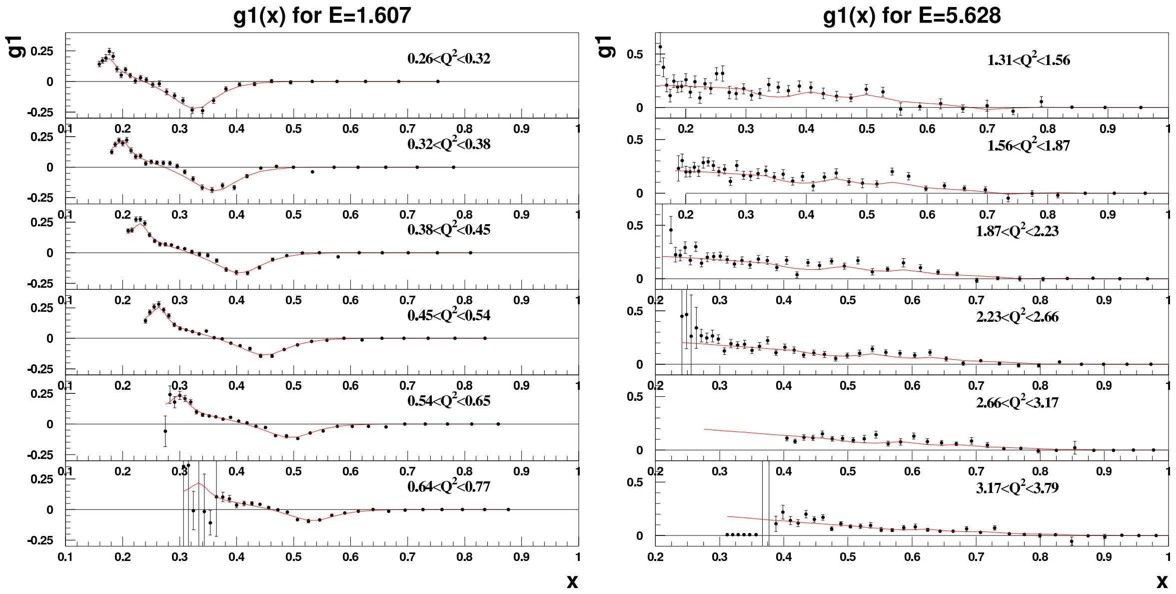

- Additional CLAS data have been taken at lower and higher energies for more complete kinematic coverage.
- For the 5.6 GeV data, g_1 is positive.
- The Δ drives the 1.6 GeV data negative.
- The newer data generally extend to lower x, and require less extrapolation when calculating moments.

CLAS (eg1b) g_1^d vs. x

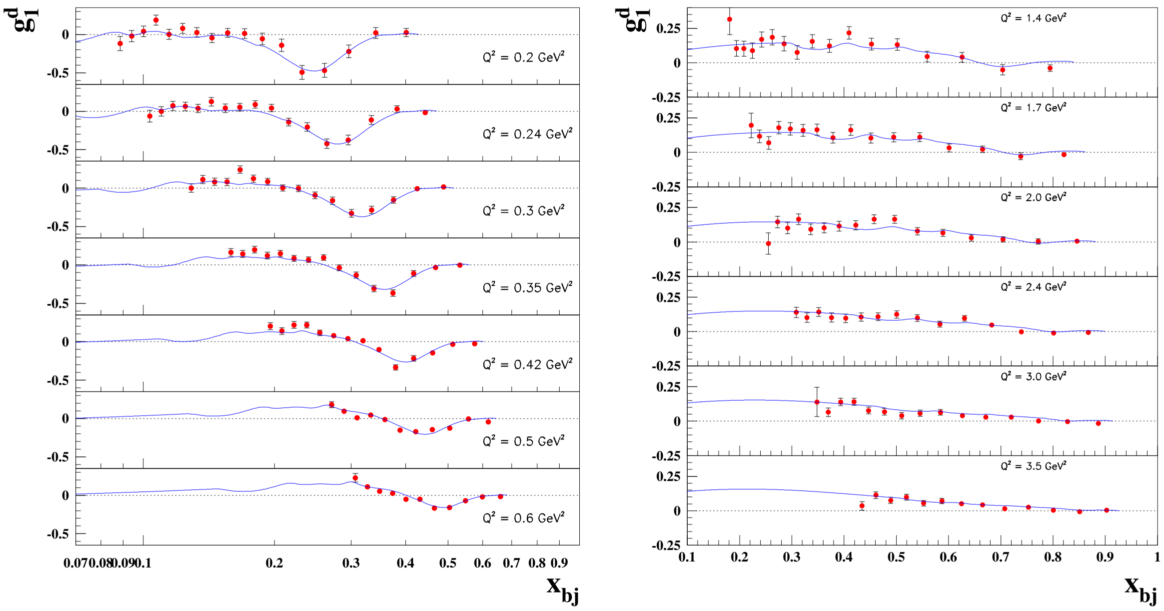

- CLAS took data with both NH_3 and ND_3 targets.
- The deuteron data show the same negative g_1 for the Δ, which disappears at higher Q^2.
- The model is a hybrid: DIS fits to data; resonance calculations using AO with helicity amplitudes modified to fit data; smooth interpolation between the two regions.

CLAS g_1/F_1

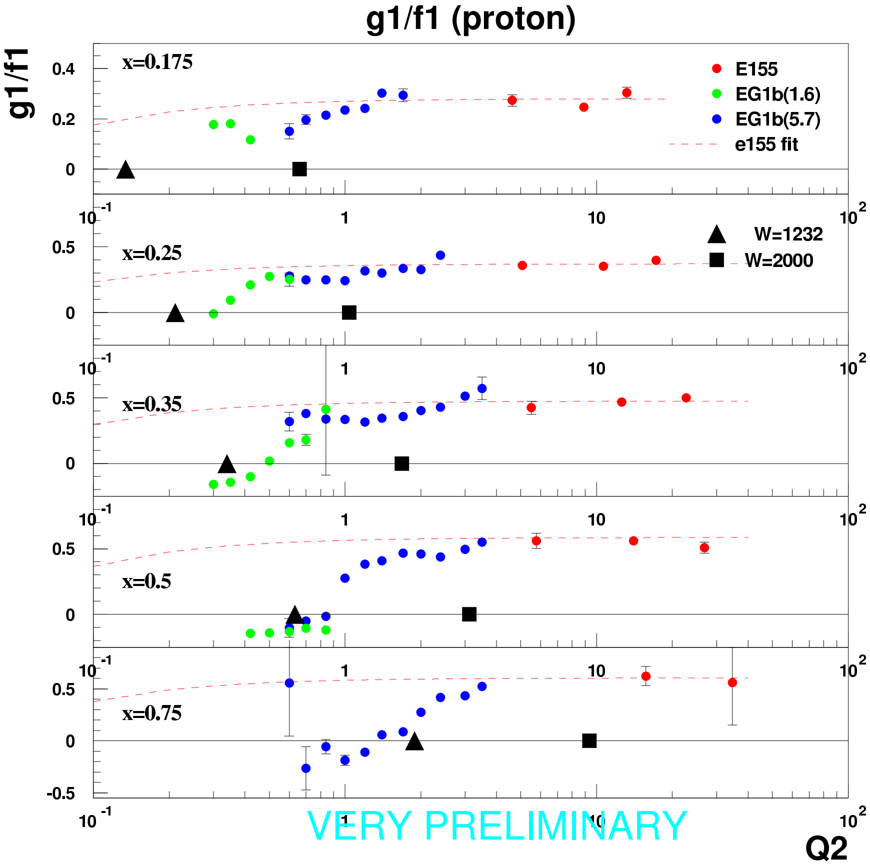

- For DIS, g_1 scales almost like F_1, and g_1/F_1 is nearly flat.
- The resonance structure causes g_1 to evolve very differently from F_1 at low Q^2.
- g_1/F_1 goes negative at the Δ resonance.

S_{11} and D_{13} Amplitudes

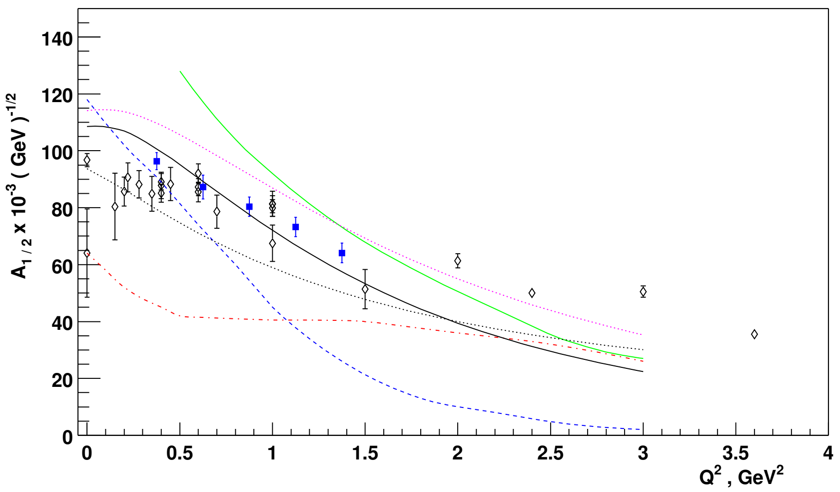

$A_{1/2}$ for the $S_{11}(1535)$ Resonance

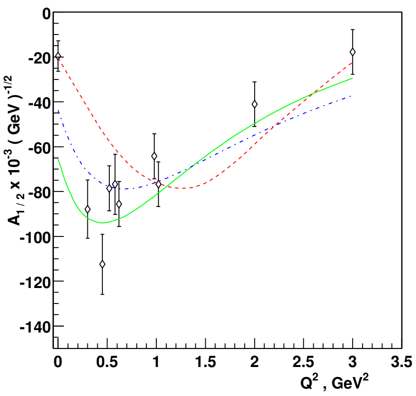

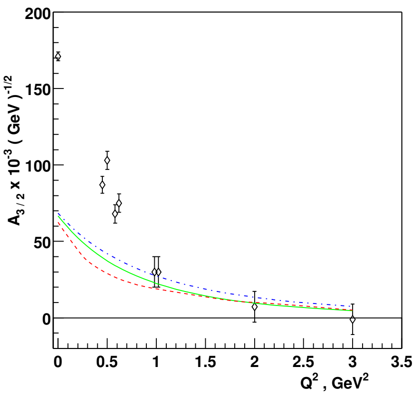

$A_{1/2}$ and $A_{3/2}$ for the $D_{13}(1520)$ Resonance

$$A_1 = \frac{|A_{1/2}|^2 - |A_{3/2}|^2}{|A_{1/2}|^2 + |A_{3/2}|^2}$$

CLAS (eg1a) $A_1 + \eta A_2$ for p

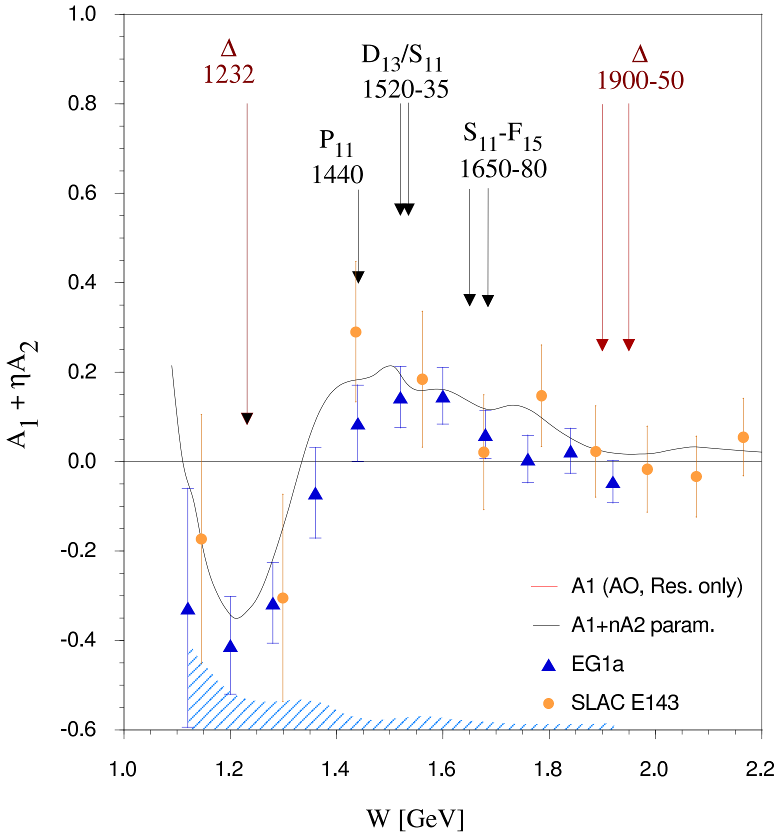

- CLAS can only measure $\|$ spin configurations.
- Therefore, $A_1 = \sigma_{TT}/\sigma_T$ cannot in general be separated from $A_2 = \sigma_{LT}/\sigma_T$.
- η is generally small, so A_1 dominates.

CLAS (eg1b) $A_1 + \eta A_2$ vs. x for p

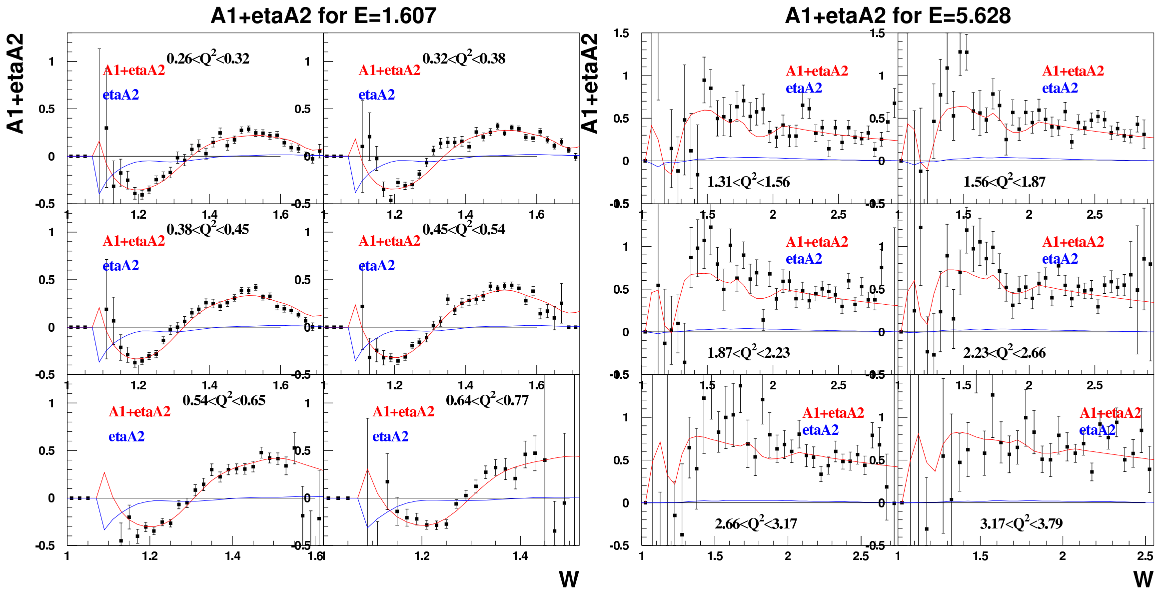

- Red curve: hybrid model
- Blue curve: estimate of ηA_2 from hybrid model.
- Plotted versus W, the data show resonance structure at fixed positions.

Hall C E01-006
Resonance Spin Structure

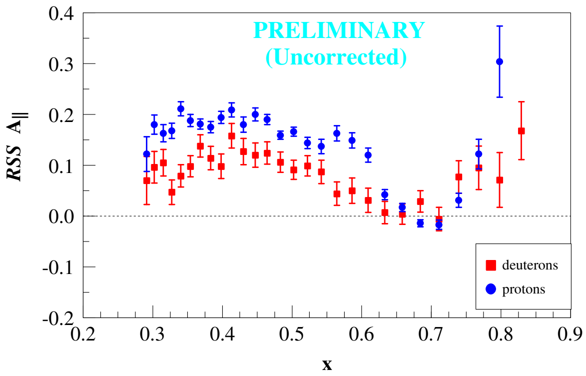

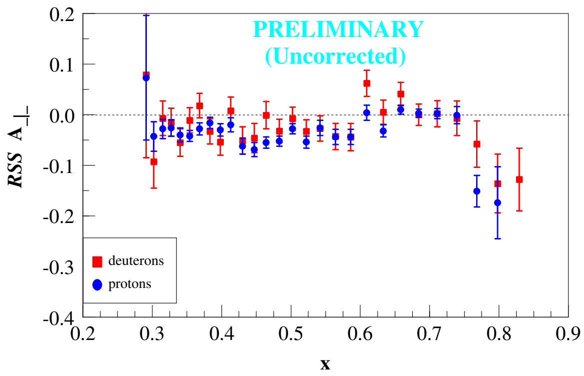

- Beam energy 5.755 GeV.
- HMS spectrometer at 13.08°.
- $< Q^2 >= 1.3$ GeV^2.
- First JLab measurement using ammonia targets to measure $\perp$ configuration.

A_1 and A_2 vs. x

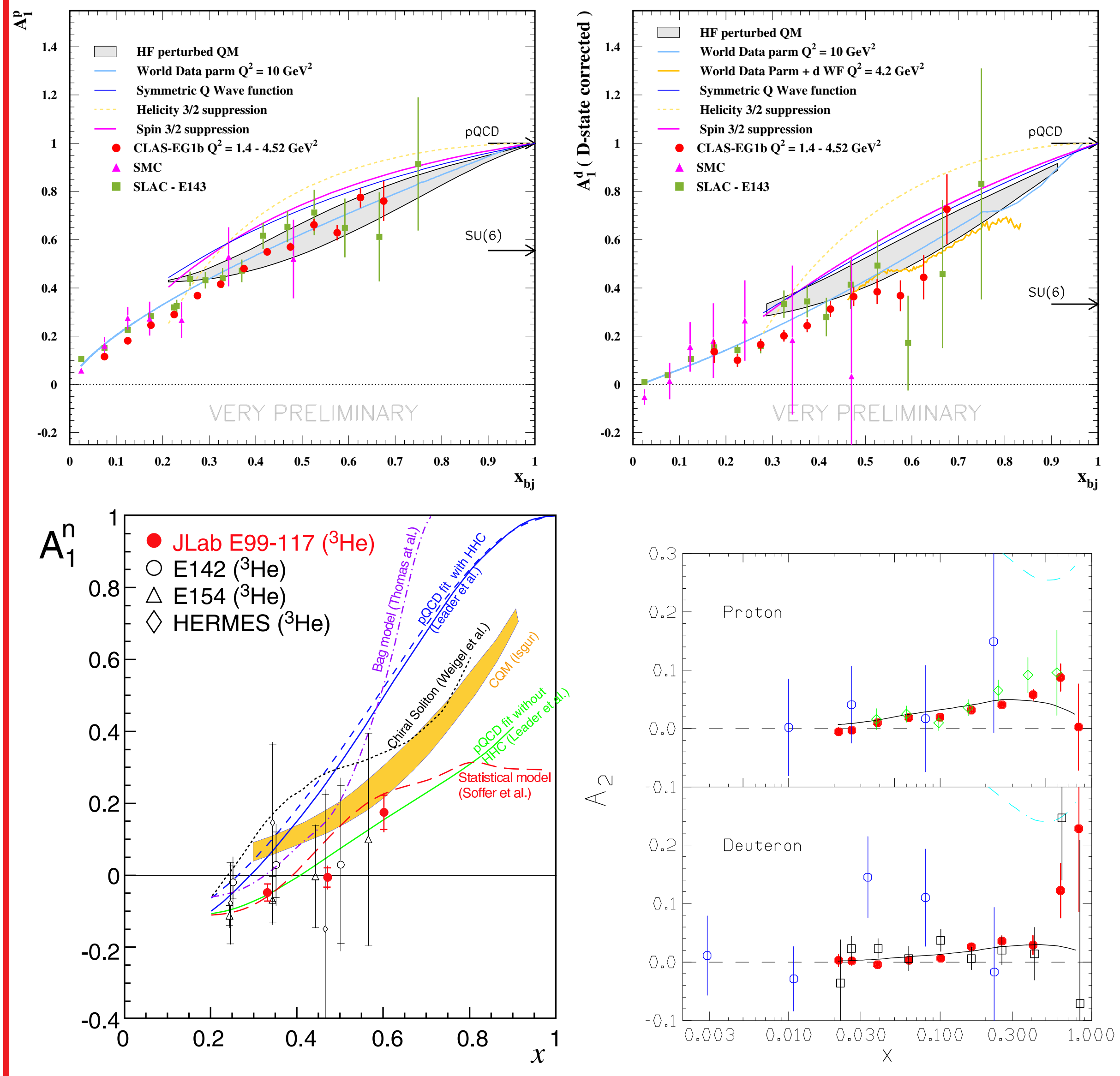

HF perturbed QM
World Data parm Q² = 10 GeV²
Symmetric Q Wave function
Helicity 3/2 suppression
Spin 3/2 suppression
CLAS-EG1b Q² = 1.4 - 4.52 GeV²
SMC
SLAC - E143
pQCD
SU(6)
VERY PRELIMINARY
x_bj
World Data Parm + d WF Q² = 4.2 GeV²
A₁^d (D-state corrected)
JLab E99-117 (³He)
E142 (³He)
E154 (³He)
HERMES (³He)
Bag model (Thomas at al.)
pQCD fit with HHC (Leader et al.)
Chiral Soliton (Weigel et al.)
CQM (Isgur)
pQCD fit without HHC (Leader et al.)
Statistical model (Soffer et al.)
Proton
Deuteron
A₂
x

SLAC E155x

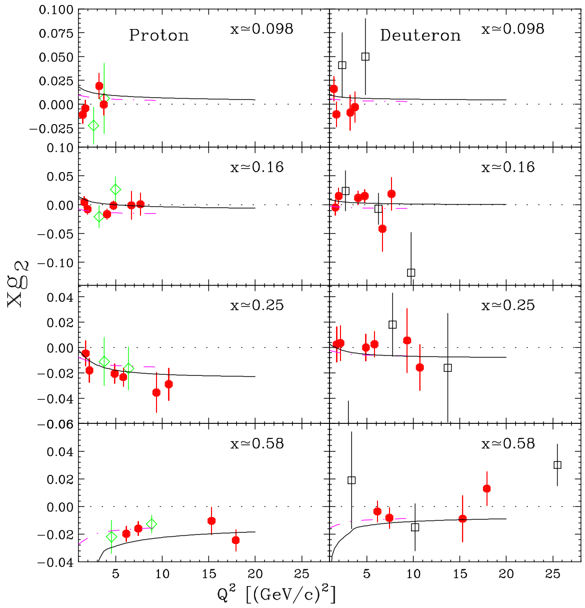

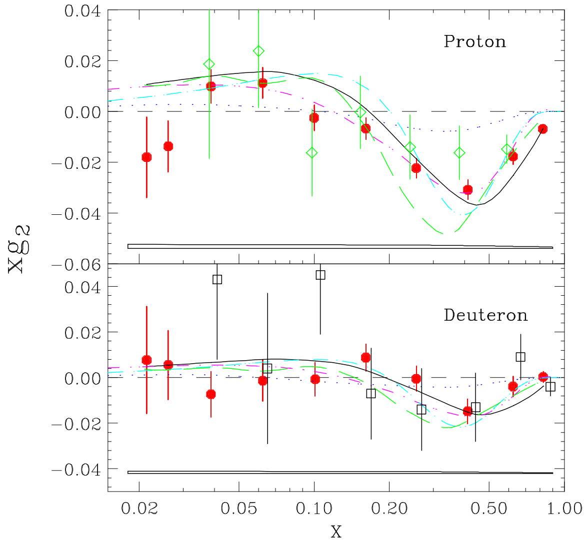

- Dedicated SLAC run to measure g_2.
- Improved on previous errors by over a factor of 3.
- $g_2^{WW} = -g_1(x, Q^2) + \int_x^1 \frac{g_1(y)}{y} dy$
- $\bar{g}_2 = g_2 - g_2^{WW}$ (higher twist component)
- Solid line shows g_2^{WW}
- Enough data exist to get a rough idea of the Q^2 evolution.

Hall A $g_1^{^3He}$ and $g_2^{^3He}$

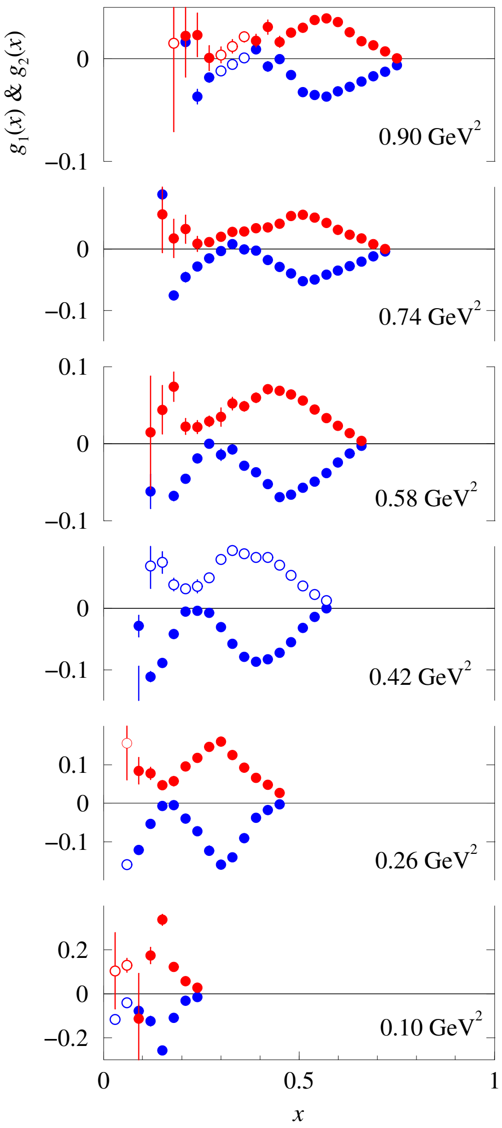

Polarized ^{3}He target enables measurement of $\|$ and $\perp$ asymmetries in the same experiment.

$g_2 \approx -g_1$
(i.e. $\sigma_{LT} \approx 0$

Hall A: E97-103

Search for Higher Twist Effects in the Neutron Structure Function $g_2^n(x, Q^2)$

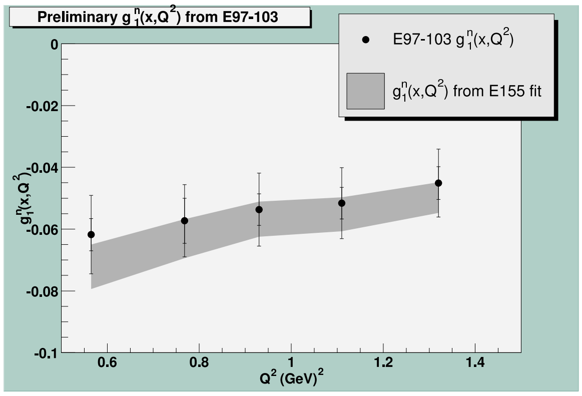

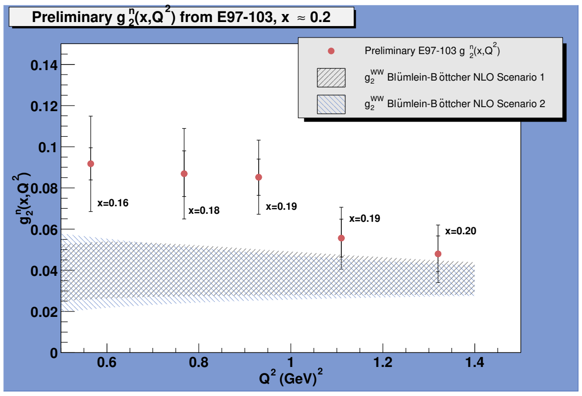

- Precision measurement of both g_1^n and g_2^n at $x \approx 0.2$ using the polarized ^{3}He target in Hall A.
- Systematics of g_1 agree with the E155 fit.
- g_2 is generally above the g_2^{WW} estimates.

Hall A E97-103

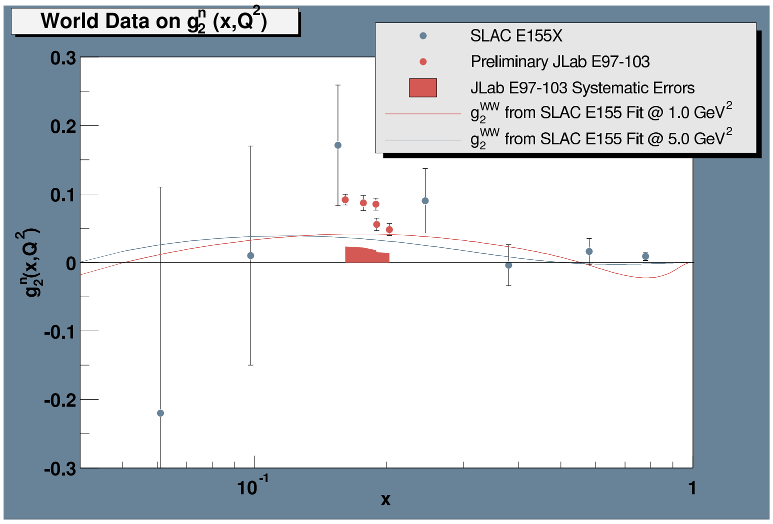

- Jlab provides unprecidented precision for structure function measurements.
- Data must be used in global analyses that include all the world's data.
- There is room for more precise data here.

Unpolarized Moments

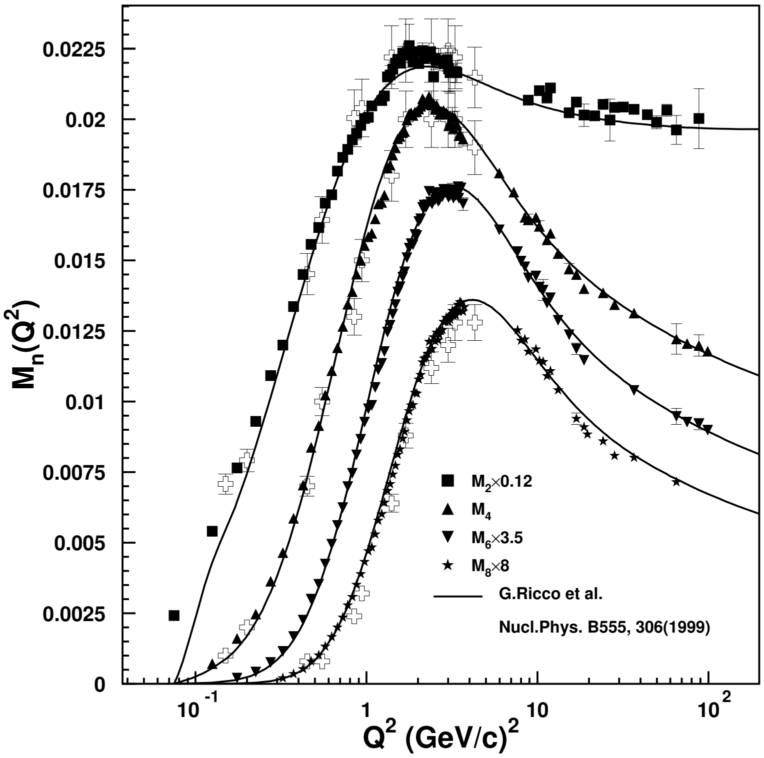

- Any function is known by its moments [e.g. $M_n = \int_0^1 dx x^n f(x)$].
- Nachtmann moments: $M_n(Q^2) = \int_0^1 dx C \frac{\xi^{n+1}}{x^3} F_2(x, Q^2)$ in which $C = [3{+}3(n_1)r{+}n(n{+}2)r^2]/[(n{+}2)(n{+}3)]$, $r = \sqrt{1 + 4M^2x^2/Q^2}$, and $\xi = 2x/(1 + r)$.
- Operator Product Expansion: $M_n(Q^2) = A_n(Q^2) + \Sigma_{k=1}^{\infty}(\frac{n\beta^2}{Q^2})^k B_{nk}(Q^2)$, in which β is the scale constant for higher twist effects.

Unpolarized Moments

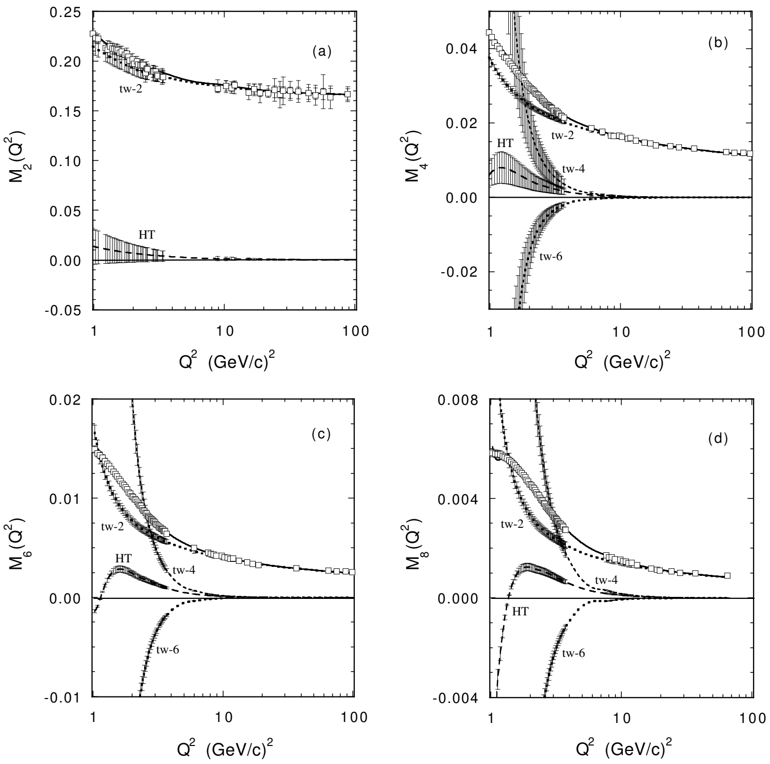

- Higher twist implies multi-parton correlations.
- Inelastic moments fit to powers of $1/Q^2$.
- Higher twist is important (especially for the higher moments) up to $Q^2 =$ 8-10 GeV^2.

CLAS Γ_1 and Γ_2 vs. Q^2

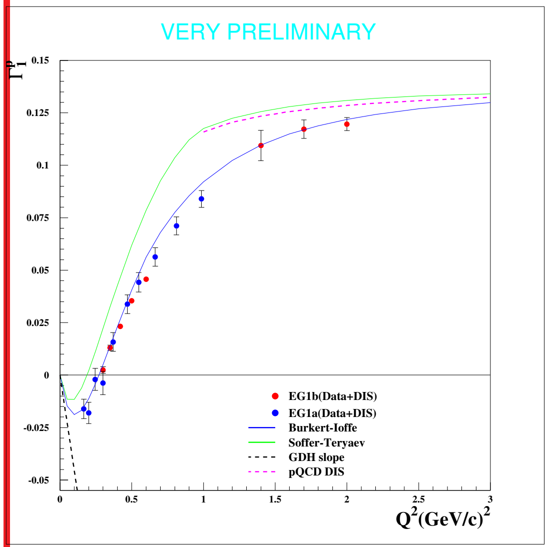

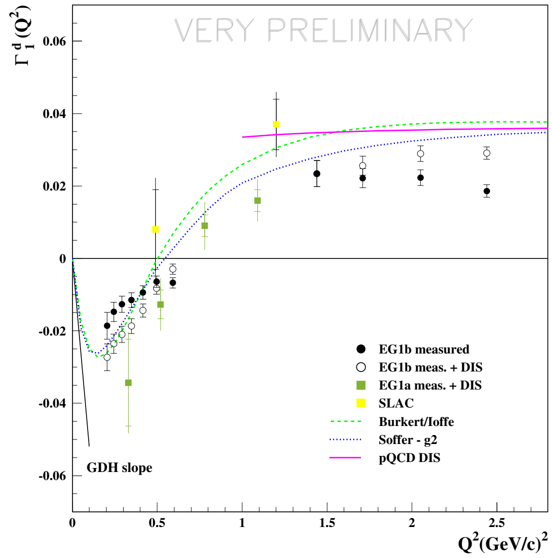

First polarized moment $\Gamma_{1,2} = \int_0^1 g_{1,2}(x, Q^2)dx$

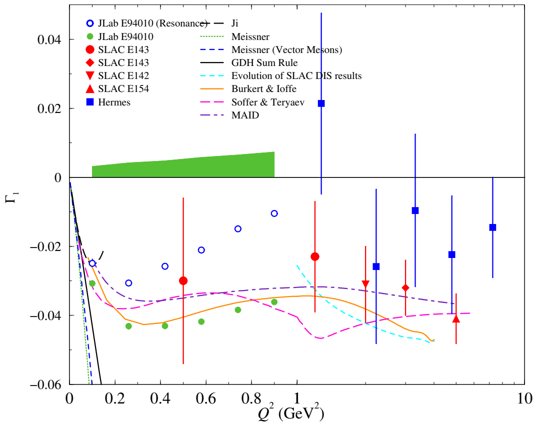

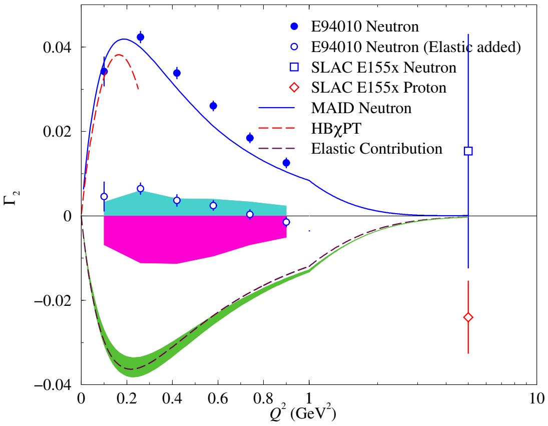

$\Gamma_1^p - \Gamma_1^n$

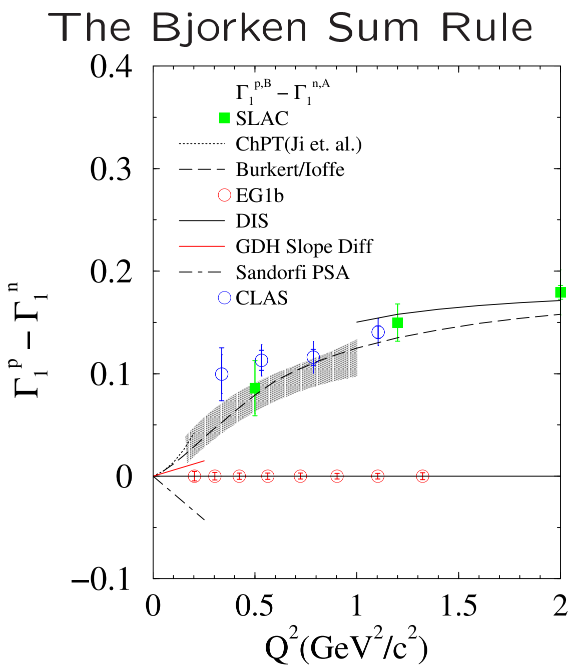

- Bjorken Sum Rule: $\Gamma_1^p - \Gamma_1^n = \frac{1}{6} g_A C_{\rm ns}$
- C_{ns} evolves with Q^2.
- At low Q^2 where resonances dominate, the pQCD extrapolation fails.
- Data are presently being analyzed that will make a precise measure of the Bjorken sum below $Q^2 \approx 1$ GeV^2.

Higher Twist Coefficient d_2

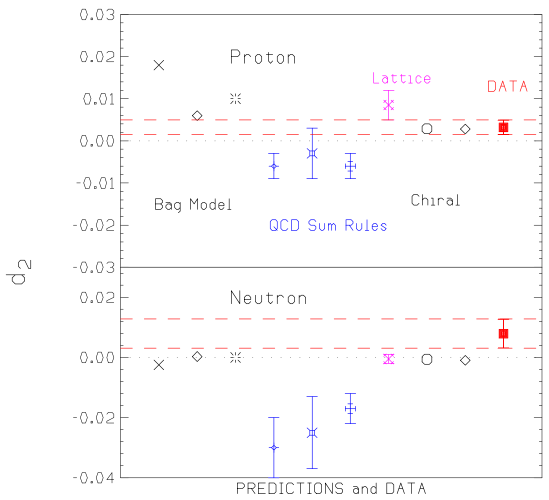

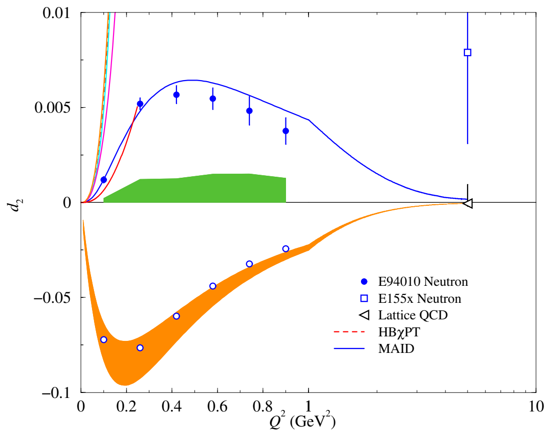

OPE up to twist-3:

$$\Gamma_1^{(n)} = \int_0^1 x^n g_1(x, Q^2) dx = \frac{a_n}{2}$$

$$\Gamma_2^{(n)} = \int_0^1 x^n g_2(x, Q^2) dx = \frac{1}{2} \frac{n}{n+1} (d_n - a_n)$$

$$d_n = 2 \int_0^1 x^n \left[g_1 + \frac{n+1}{n} g_2 \right] dx$$

Future GDH Measurements

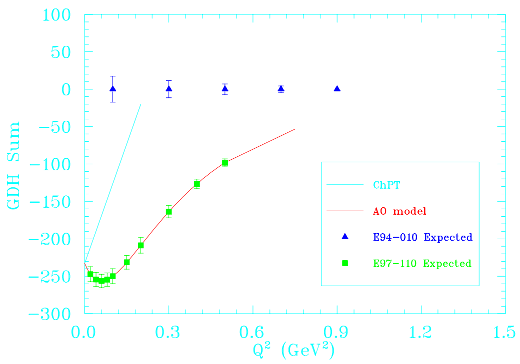

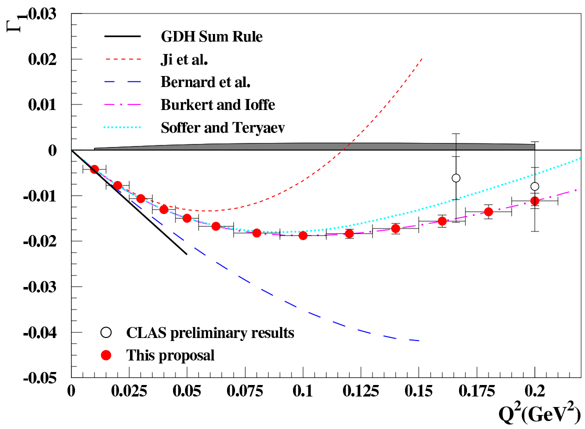

- Hall A will extend its polarized neutron structure function measurements to low Q^2 by using a septum magnet to get down to 6° scattering angles (left graph).
- Hall B will extend its polarized proton structure function measurements to low Q^2 by using a new small-angle Cherenkov counter (right graph).
- Together, these experiments will map out the approach to the Gerasimov-Drell-Hearn (GDH) limit.
- GDH extrapolation shows $\Gamma_1 \to -\kappa^2 Q^2/8M^2$ as $Q^2 \to 0$.

Conclusions

- Jlab results show exceptional precision and kinematic coverage for both unpolarized and polarized structure functions in the resonance region and beyond.
- Proper understanding in the framework of QCD requires an expansive data set for which the determination of moments of structure functions can be done without excessive extrapolation. This is now possible with JLab data.
- These high-quality data from JLab provide the framework for understanding the complex region between chiral and QCD perturbative descriptions.
- With the upgrade in energy and new techniques for measuring the neutron, JLab can effectively provide a complete set of data at low Q^2 that ties directly to the world's DIS data.

Hall A

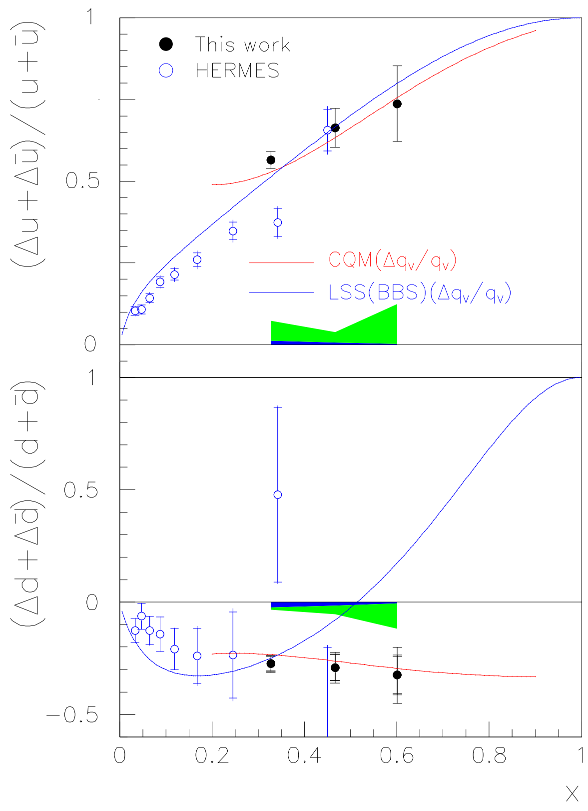

Assume no strange quarks for $x > 0.3$ and no Q^2-dependence of A_1

$$\frac{\Delta u}{u} = \frac{4}{15}\frac{g_1^p}{F_1^p}(4+R) - \frac{1}{15}\frac{g_1^n}{F_1^n}(1+4R)$$

$$\frac{\Delta d}{d} = \frac{4}{15}\frac{g_1^n}{F_1^n}(4+1/R) - \frac{1}{15}\frac{g_1^p}{F_1^p}(1+4/R)$$

$$R \equiv d/u$$

CLAS Polarized Target

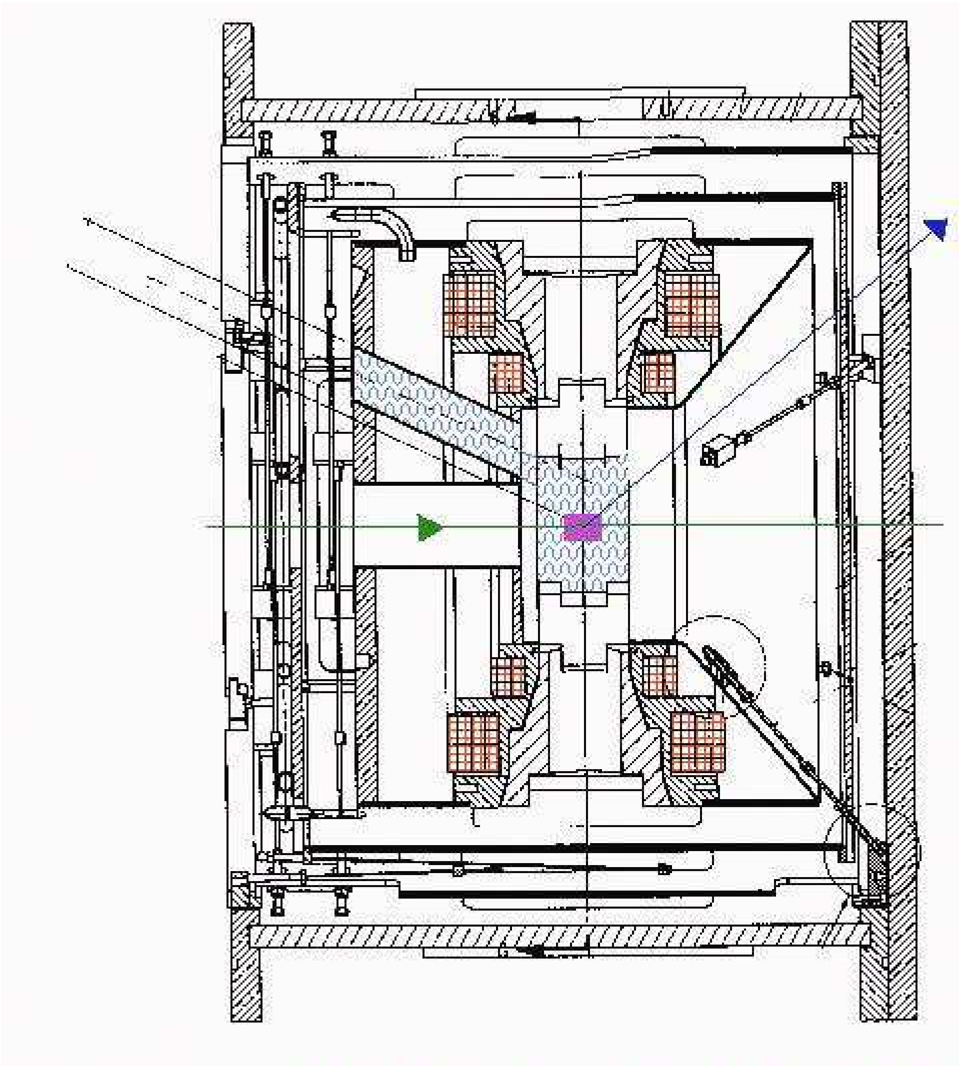

- Targets of $^{15}NH_3$ and $^{15}ND_3$, 1 cm long, 1.5 cm diameter; 1 K, 5 T field, dynamic nuclear polarization.
- $P_t \approx$ 50–80% for proton; $P_t \approx$ 10–35% for deuteron.

Hall A Polarized Target

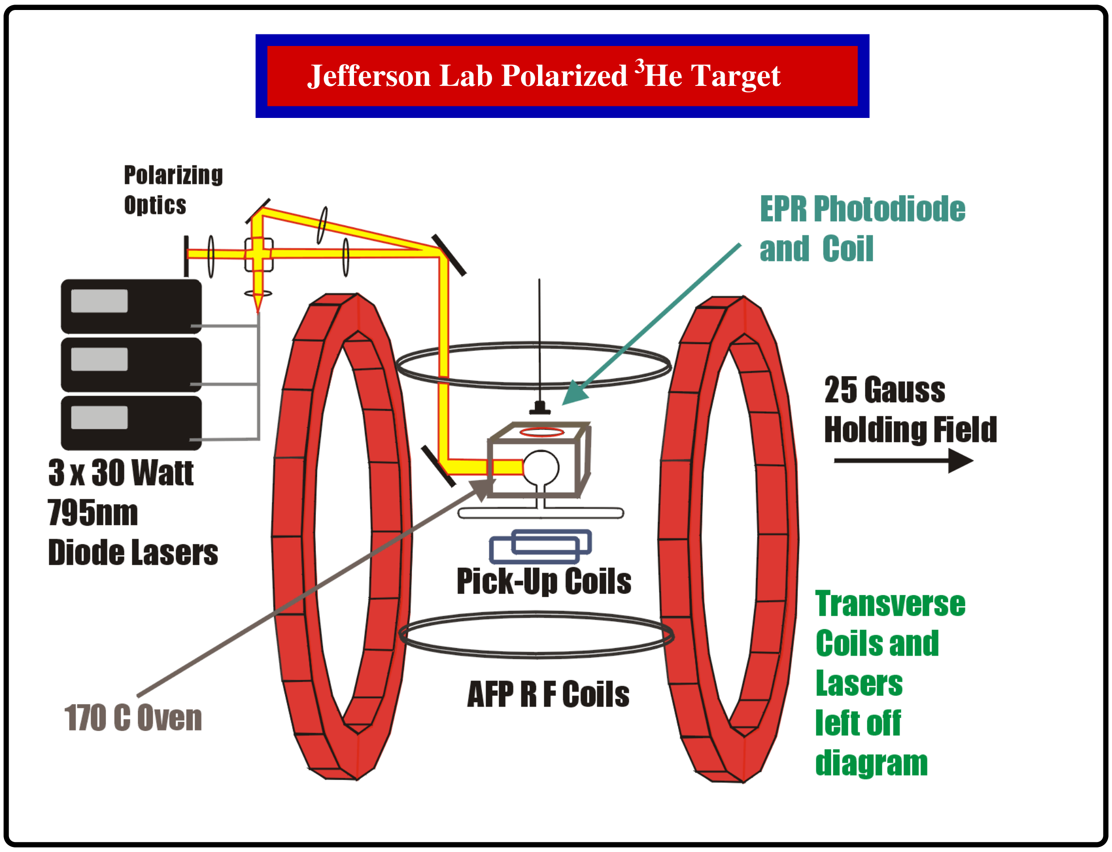

Kinematic Coverage